
01 Apr 1999

Atomic Structure and Magnetism of Ordered and Disordered $\text{Al}_{0.5}\text{Fe}_{0.5-x}\text{Mn}_x$ Alloys

V. G. Harris

D. J. Fatemi

K. B. Hathaway

Q. Huang

et. al. For a complete list of authors, see https://scholarsmine.mst.edu/chem_facwork/934

Follow this and additional works at: https://scholarsmine.mst.edu/chem_facwork

 Part of the [Chemistry Commons](#)

Recommended Citation

V. G. Harris et al., "Atomic Structure and Magnetism of Ordered and Disordered $\text{Al}_{0.5}\text{Fe}_{0.5-x}\text{Mn}_x$ Alloys," *Journal of Applied Physics*, vol. 85, no. 8, pp. 5181-5183, American Institute of Physics (AIP), Apr 1999. The definitive version is available at <https://doi.org/10.1063/1.369117>

This Article - Journal is brought to you for free and open access by Scholars' Mine. It has been accepted for inclusion in Chemistry Faculty Research & Creative Works by an authorized administrator of Scholars' Mine. This work is protected by U. S. Copyright Law. Unauthorized use including reproduction for redistribution requires the permission of the copyright holder. For more information, please contact scholarsmine@mst.edu.

Atomic structure and magnetism of ordered and disordered $\text{Al}_{0.5}\text{Fe}_{0.5-x}\text{Mn}_x$ alloys

V. G. Harris,^{a)} D. J. Fatemi, and K. B. Hathaway
U.S. Naval Research Laboratory, Washington, DC 20375

Q. Huang

National Institute of Standards and Technology, NIST Center for Neutron Research, Gaithersburg, Maryland 20899 and Department of Materials and Nuclear Engineering, University of Maryland, College Park, Maryland 20742

Amitabh Mohan and Gary J. Long

Department of Chemistry, University of Missouri-Rolla, Rolla, Missouri 65409-0010

The equiatomic FeAl alloy has been modified by partial substitution of Mn for Fe, and its magnetic and structural properties investigated by neutron diffraction (ND), x-ray absorption fine structure (XAFS) spectroscopy, Mössbauer spectroscopy (MS), and SQUID magnetometry both for the ordered ($B2$) and disordered states. The unit cell volume is measured to increase linearly with Mn concentration. XAFS measurements indicate local structural displacements occur at the Mn sites in both ordered and disordered states that may act to frustrate long-range magnetic order (LRMO). Although MS and ND show no evidence of LRMO, SQUID magnetometry indicates an induced movement in the ordered state that increases with disorder but does not saturate at fields up to 5 T. © 1999 American Institute of Physics. [S0021-8979(99)15408-2]

Although magnetism in FeAl alloys has been investigated extensively over many years, it is not yet clear whether their complex magnetic behavior is better described by itinerant or local exchange interactions. Increasing substitution of Al into bcc Fe is known to produce an ordered $B2$ phase, with the Al atoms all on the same cubic sublattice, from a few percent Al until the ordered CsCl structure is reached for FeAl. The magnetic moment decreases proportionally to the amount of Al dilution up to about 20 at%, then falls off rapidly, going to zero at 35% Al.¹ Antiferromagnetism was proposed to explain the lack of ferromagnetism, and the observed high field susceptibilities for alloys with greater than 33% Al,² but antiferromagnetic order was not observed by polarized neutron experiments.^{3,4} However, local antiferromagnetic interactions have been used to explain the behavior of low temperature magnetoresistance in FeAl.⁵

The relatively short second near neighbor spacings between Fe-Fe pairs argue for some degree of itinerancy and magnetic order due to d electron overlaps (the same overlaps which give strong negative second neighbor exchange interactions in bcc Fe). On the other hand, a statistical model based in its simplest form on local moments has been used successfully to describe the magnetization produced in alloys with greater than 30% Al by the intentional introduction of disorder.⁶ Cold worked disordered samples show ferromagnetism up to the 50-50 FeAl composition with the moment falling rapidly to zero for more Al-rich alloys.⁶

Working from an itinerant rigid-band picture we have tried to push the equiatomic FeAl alloy toward magnetic ordering by substituting manganese for iron. Mn is almost midway between Fe and Al in size (atomic radii for Fe, Mn, and Al are 1.26, 1.35, and 1.43 Å, respectively) so it might

be expected to expand the lattice and narrow the d bands, enhancing the tendency toward exchange splitting of these bands. Mn, with one fewer d electron than Fe, should also move the Fermi level to lower energy more toward the center of the d band density of states. Recent band structure calculations,⁷ which predict only weak ferromagnetism for FeAl, indicate that this would place the Fermi energy in a region of higher density of states, also increasing the tendency toward magnetic ordering.

Pseudobinary alloys of $\text{Al}_{0.5}\text{Fe}_{0.5-x}\text{Mn}_x$ ($x=0.05, 0.1, 0.15$) were arc melted (AM) from elemental constituents having 99.99% purity or better. Equal portions of the arc-melted alloys were annealed (ANN) at 800 °C for 8 h to promote further chemical order, or high-energy ball milled (BM) for a period of 5 h (in air) to promote chemical disorder. These samples were characterized using neutron diffraction, x-ray absorption fine structure (XAFS) spectroscopy, Mössbauer spectroscopy (MS) SQUID magnetometry to determine their long-range-order properties, element-specific atomic structure, and local magnetic properties, respectively.

The neutron powder diffraction intensity data were collected using the BT-1 high-resolution powder diffractometer located at the reactor of the NIST Center for Neutron Research. A Cu (311) monochromator was employed to produce a monochromatic neutron beam wavelength of 1.5401(1) Å. Collimators with horizontal divergences of 15', 20', and 7' of arc full width at half maximum were used before and after the monochromator, and after the sample, respectively. The intensities were measured in steps of 0.05° in the 2θ range 3°-168°. Data were collected at room temperature for all samples and at 8 K for the $x=0.1$ ball-milled sample to elucidate the structure and to detect any possible magnetic ordering. The structure refinements were carried out with the Rietveld profile fitting method using the pro-

^{a)}Electronic mail: harris@anvil.nrl.navy.mil

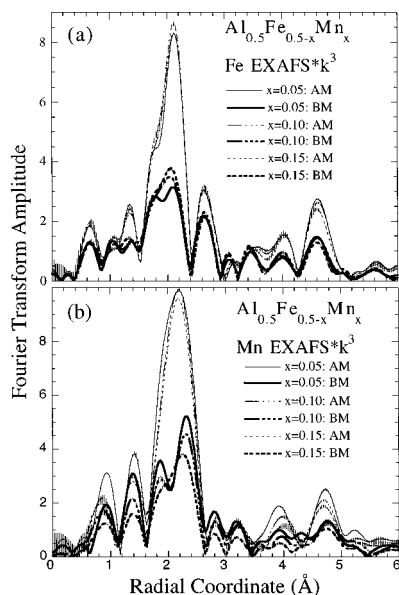


FIG. 1. (a) Fourier transformed Fe EXAFS data for arc-melted (AM) and ball-milled (BM) samples. A k range of $3\text{--}14 \text{ \AA}^{-1}$ with a k^3 weighting was employed in the Fourier transformation. (b) Fourier transformed Mn EXAFS data for AM and BM samples. A k range of $3\text{--}12 \text{ \AA}^{-1}$ with a k^3 weighting was employed in the Fourier transformation. Error bars on the data reflect both the data collection statistics and the uncertainty introduced to the data from the procedural steps leading to and including the Fourier transformation.

gram GSAS.⁸ The neutron scattering amplitudes used in the calculations are 0.345, 0.954, and $-0.344 (\times 10^{-12} \text{ cm})$ for Al, Fe, and Mn, respectively.

XAFS measurements were performed on the NRL beamline, X23B, at the National Synchrotron Light Source (Brookhaven National Laboratory). XAFS data collection was performed in transmission mode under ambient conditions. The extended fine structure was analyzed using standard procedural steps⁹ leading to the Fourier transformation of the data to radial coordinates.

The Mössbauer spectra were obtained on a constant-acceleration spectrometer which used a room temperature rhodium matrix Co^{57} source and was calibrated at room temperature with $\alpha\text{-Fe}$ foil. Spectra were fit using the method of Le Caer¹⁰ in which a linearly correlated distribution between the isomer shift and the quadrupole splitting is given by: $\delta = a(\Delta EQ) + b$, where a is unitless and b is in mm/s. The fits use 20 component doublets each of which has a linewidth of 0.23 mm/s, the instrumental linewidth of the spectrometer.

Magnetic measurements were performed at temperatures ranging from 5 to 300 K and at fields of 0–5 T using SQUID magnetometer.

Rietveld analysis of the powder neutron diffraction patterns acquired for the AM samples reveals pure phase alloys that are approximately 98% chemically ordered where (Fe, Mn) and Al exist in a CsCl-type structure (space group: $Pm3m$). Significant particle broadening was observed for the ball-milled samples. Unit cell volumes are found to increase linearly with increasing Mn content from 24.995 \AA^3 for $x=0.05$ to 25.369 \AA^3 for $x=0.15$. After a heat treatment at 800°C for a period of 8 h, the ordering improved to 99% and the unit cell volume increased by approximately 0.3%.

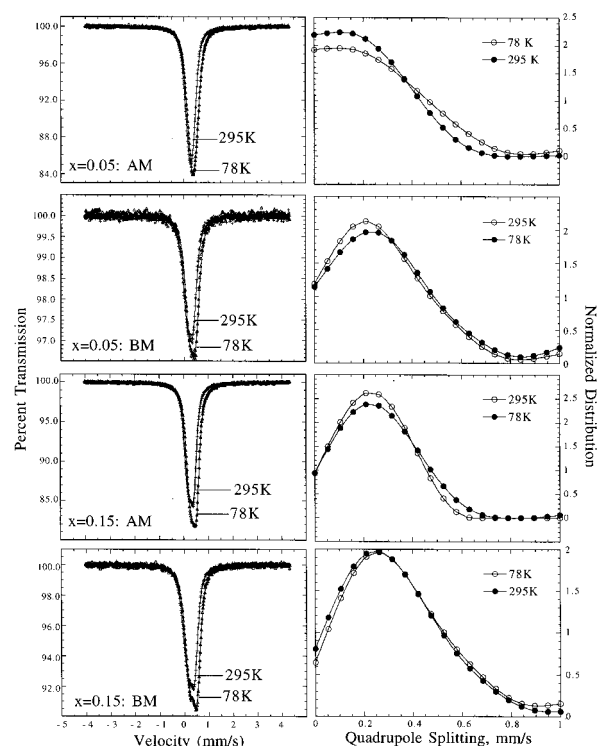


FIG. 2. Mössbauer spectra collected for the $x=0.05$ and $x=0.15$ samples after arc-melting and ball-milling at 78 and 295 K. On the right-hand side of the figure are the quadrupole splitting distributions.

The ball milling acted to reduce the chemical order to $<5\%$, while the unit cell volume increased 0.9% from the arc-melted state. No evidence of either ferro- or antiferromagnetic long-range order was observed in the neutron diffraction experiments.

Fourier transformed (FT) Fe and Mn K EXAFS collected from all AM and BM samples are presented in Figs. 2 and 3, respectively. The environment of the Fe atoms in the AM samples show characteristics of a body-centered structure, namely the near-neighbor (NN) peak centered $\sim 2.05 \text{ \AA}$ and the next near neighbor (NNN) (i.e., lattice parameter site) centered $\sim 2.65 \text{ \AA}$. These values are offset from their true bond distances (calculated at 2.539 and 2.932 \AA , respectively) by a unique electron phase shift intrinsic to XAFS. The slight shoulder appearing on the low r side of the NN peak may be an artifact of the Fourier transformation, or in

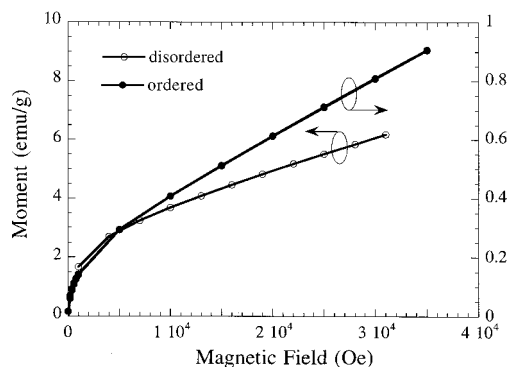


FIG. 3. Magnetization vs applied field for the $\text{Al}_{0.5}\text{Fe}_{0.45}\text{Mn}_{0.05}$ alloy in the ordered and disordered states.

fact may signal a splitting of the NN shell from a local distortion. The FT profile for the Fe atoms does not change appreciably with increasing Mn content. Similar data collected from the BM samples are plotted on the same axes of this plot. The amplitude of the FT peaks for these samples is greatly reduced due to the reduction in chemical order and the introduction of static spatial disorder. One profound development is the splitting of the NN peak. This is too large to be an artifact and must be interpreted as arising from a bimodal distribution of NN bonds. Such a bimodal distribution may arise from the dilation or contraction of bonds between like and unlike atom pairs. Because the neutron diffraction did not reveal any distortion of the cubic unit cell, this local distortion is not translated to the average periodic structure.

In comparing the FT Mn EXAFS data to the Fe data of Fig. 1 one sees that the NN and NNN peaks are not resolved in the Mn profiles but are instead incorporated into a very large broad peak centered ~ 2.1 Å. This is also the reason that the amplitude of this peak is larger than the NN peak in the Fe FT profiles. The peak centered near 4.6 Å in both the Fe and Mn profiles is a signature peak of a body-centered cubic structure and arises in part both from direct scattering events between the absorber and the body-diagonal site, and from multiple scattering MS events from the collinear arrangement between the absorber, body-centered, and body-diagonal atoms. This peak amplitude is reduced in the Mn data relative to the Fe. One possible explanation for this is that the collinear MS amplitude is diminished in the Mn environment due to either isotropic strain or atomic displacements in its local environment.

When one considers only the Mn data of Fig. 2 one sees that the general features of the profile do not change appreciably with Mn content. After ball milling the average Mn environment experiences a large amplitude reduction which is similar to that of Fe in Fig. 1. The NN peak of the Mn profile reveals a pronounced splitting which results from increased atomic disorder with increasing Mn content. This splitting can be attributable to a large local tetragonal distortion around the Mn sites or to local bond contraction and dilation similar to that proposed for the Fe data in Fig. 1.

Figure 3 is a plot of Mössbauer spectra collected for the $x=0.05$ and 0.15 alloys in the AM and BM states. The corresponding quadrupole splitting distributions are presented on the right hand side of Fig. 3. All of the remaining spectra were virtually identical in appearance to those shown in Fig. 3 and none of the samples exhibit the presence of any magnetic order between 295 and 78 K. For all the compounds the average isomer shifts and their temperature dependence are typical of these alloys and systematically increase in the order ball-milled < arc melted < annealed. The increase is real and corresponds to a significant decrease in the s electron density at the iron-57 nucleus in the order ball milled < arc melted < annealed. These changes must reflect short-range changes in the local bonding environment at the iron because there is no correlation with the changes in the unit cell volume. Further there are no differences observed for the differing amounts of Mn present. As expected, the average quad-

rupole splitting increases on cooling. There is no systematic trend with the amount of Mn present, but for all three different amounts of Mn present the average quadrupole splitting decreases in the order: ball milled > arc melted > annealed. Again this is a real and significant increase and indicates, as expected, that the local site symmetry at the iron is the most symmetric in the annealed samples, less symmetric in the arc melted samples, and least symmetric in the milled samples.

From the linear correlation between the average isomer shift and the quadrupole splitting, as expected for a cubic material, the intercept corresponding to the average quadrupole splitting is ~ 0 mm/s. This follows from the normal behavior of the isomer shifts and the uniform trend in the average quadrupole splitting.

Magnetization versus applied field measurements were collected at 300 K for the $\text{Al}_{0.5}\text{Fe}_{0.45}\text{Mn}_{0.05}$ sample before and after ball milling (see Fig. 3). The magnetization does not achieve saturation in fields up to 5 T. The magnetization of the milled, or disordered, sample is nearly an order of magnitude larger than the precursor. This is likely due to the increase in magnetic near neighbors and next near neighbors. It is interesting to note that the $\text{Al}_{0.5}\text{Fe}_{0.5}$ alloy has been reported to be nonmagnetic at all temperatures^{3,4} and becomes ferromagnetic only after cold working.⁶ In this case, we have shown that even small amounts of Mn substitution for Fe are effective in providing the system an enhanced susceptibility. In the disordered state none of the alloys studied here are ferromagnetic but exhibit some degree of enhanced susceptibility with a larger moment than the ordered alloys. Experiments to better understand the enhanced susceptibility in these substituted alloys are in progress.

In summary, our attempt to produce a magnetically ordered alloy by substitution of up to 30% Mn for Fe in ordered and disordered FeAl alloys was unsuccessful, as the Mössbauer and neutron diffraction results do not show either ferromagnetic or antiferromagnetic order. A possible reason for this is the introduction of local atomic displacements around both Fe and Mn sites as indicated by the shifts in NN peaks shown in the EXAFS results. These local distortions are much more pronounced after ball milling. Experiments to determine if there is enhanced susceptibility in these substituted alloys are in progress.

¹ *Landolt-Bernstein New Series*, edited by H. P. J. Wijn (Springer, Berlin, 1987), Vol. III 19b, pp. 295–356.

² A. Arrott and H. Sato, *Phys. Rev.* **114**, 1420 (1959).

³ F. Nathans and S. J. Pickart, in *Magnetism*, edited by G. T. Rado and H. Suhl (Academic, New York, 1963), Vol. III.

⁴ P. A. Oles, *Acta Phys. Pol.* **27**, 343 (1965).

⁵ G. R. Caskey, J. M. Franz, and D. J. Sellmyer, *J. Phys. Chem. Solids* **34**, 1179 (1973).

⁶ M. J. Besnus, A. Herr, and A. J. P. Meyer, *J. Phys. F* **5**, 2138 (1975).

⁷ D. J. Singh, in *Intermetallic Compounds: Principles*, edited by J. H. Westbrook and R. L. Fleisher (Wiley, New York, 1994), Vol. I.

⁸ A. C. Larson and R. B. Von Dreele, "General Structure Analysis System," Los Alamos National Laboratory, Rep. No. LAUR086-748 (1990).

⁹ D. E. Sayers and B. A. Bunker, in *X-ray Absorption: Principles, Applications, Techniques of EXAFS, SEXAFS, and XANES*, edited by D. C. Koningsberger and R. Prins (Wiley, New York, 1988), Vol. 92, pp. 211–253.

¹⁰ G. Le Caer and J. M. Dubois, *J. Phys. E* **12**, 1083 (1979).